JOURNAL OF MATERIALS SCIENCE 30 (1995) 1245–1250

Nonstoichiometry and physical properties of the perovskite $Ba_xLa_{1-x}FeO_{3-y}$ system

K. S. ROH, K. H. RYU, C. H. YO
Department of Chemistry, Yonsei University, Seoul 120-749, Korea

A series of samples in the $Ba_xLa_{1-x}FeO_{3-y}$ system ($x = 0.00, 0.25, 0.50, 0.75$, and 1.00) have been prepared at 1200 °C under an atmospheric air pressure. The solid solutions of the system were analysed from the X-ray diffraction spectra and thermal analyses. X-ray diffraction studies assigned the compositions of the $x = 0.00$ and 1.00 to the orthorhombic system and the compositions of the $x = 0.25, 0.50$, and 0.75 to the cubic system. The reduced lattice volume increased with the x value in the system. The mole ratios of the Fe^{4+} ion in the solid solutions, or τ values, were determined by Mohr salt analyses and the non-stoichiometric chemical formulae of the system were formulated from the x, τ, and y values. From the results of the Mössbauer spectroscopy, the coordination and the magnetic property of the iron ion have been discussed. The electrical conductivities were measured as a function of temperature under atmospheric air pressure. The activation energy was minimum at the composition of $x = 0.50$. The conduction mechanism can be explained by the hopping model between the mixed valences of the Fe^{3+} and Fe^{4+} ions.

1. Introduction

There have been many studies [1–6] of the magnetic and electrical properties of perovskite-type oxides which are structurally related to the mineral perovskite, $CaTiO_3$. The oxides have the ability to stabilize cations in unusually high oxidation states, and the anion sublattice can accommodate a high concentration of vacant sites. These compounds are useful in many fields such as laser host materials, thermisters, semiconductors, capacitors, superconductors, etc.

The orthoferrites [7, 8] have the formula $RFeO_3$ of which R is a rare-earth metal. Their space group is $P_{bnm}(D_{2h}^{16})$ and thus the unit cell contains four equivalent iron ions. The distortion of the perovskite structure is such that the iron environment remains essentially octahedral but the octahedra are tilted out of a c-axis. The angle of tilting is determined to a large extent by the size of the R ions. The larger the R ions, the more the chain stretches, the angle decreases and the superexchange bond angle approaches 180°. Thus $LaFeO_3$ with G-type magnetic structure has the highest Néel temperature of 750 K and $LuFeO_3$ has the lowest Néel temperature of 623 K.

Mizusaki *et al.* [9, 10] have investigated a $LaFeO_3$ system in which electrical conduction is found to be n-type in the lower P_{O_2} range and p-type in a higher P_{O_2} range. The carrier mobility calculated from the conductivity and the Seebeck coefficient suggests a hopping-type conduction mechanism.

$BaFeO_{3-y}$ [11–13] has different phases from $CaFeO_{3-y}$ and $SrFeO_{3-y}$ due to the larger size of the barium ion. There is the cubic perovskite phase for $y = 0.00$, the hexagonal phase for $0.07 \leqslant y \leqslant 0.35$, the orthorhombic phase for $0.44 \leqslant y \leqslant 0.46$, and the monoclinic phase for $y = 0.50$ [14]. The hexagonal structure of the $BaFeO_{2.79}$ [15] is similar to structure of the $BaTiO_3$: in the latter's structure, two out of three titanium cations form pairs sharing a common octahedral site face and one out of three titanium cations shares only a common octahedral site corner, as in the perovskite structure. Thus the interaction between iron ions is weak and the Néel temperature is low. The oxygen vacancies are mainly distributed in the shared faces. In the monoclinic phase of $BaFeO_{2.50}$, the unit cell contains 28 perovskite subunit cells in which the octahedral sites are linked by sharing corners and the superexchange interaction between iron ions is more favourable. The compound is an antiferromagnetic one with a Néel temperature of 720 K. Oxygen vacancies of the $BaFeO_{2.50}$ are randomly distributed, although they are ordered in the brownmillerite structures of the $CaFeO_{2.50}$ and $SrFeO_{2.50}$.

In the study of $BaLaFe_2O_{5.91}$, Battle *et al.* [16] and Parras *et al.* [17] suggest that the crystal system is cubic and the space group is $Pm3m$. Its magnetic property is consistent with simple G-type antiferromagnetism. The average magnetic moment per iron atom is 1.87 μ_B. The magnetic hyperfine splitting disappears at 240 K.

In the present study, the solid solutions of the $Ba_xLa_{1-x}FeO_{3-y}$ ($x = 0.00, 0.25, 0.50, 0.75$, and 1.00) system have been prepared and their structures were analysed by the X-ray diffraction (XRD). The amount of Fe^{4+} ion or the mixed valence state between Fe^{3+} and Fe^{4+} ions was determined by Mohr salt titration.

0022–2461

The non-stoichiometric chemical formula for the $Ba_xLa_{1-x}Fe^{3+}_{1-\tau}Fe^{4+}_{\tau}O_{3-y}$ system have been determined. The magnetic and electrical properties will be discussed with non-stoichiometric compositions.

2. Experimental procedure

2.1. Sample preparation

The solid solutions of the $Ba_xLa_{1-x}FeO_{3-y}$ system for the compositions of $x = 0.00$, 0.25, 0.50, 0.75, and 1.00, were prepared with the starting materials such as La_2O_3, $BaCO_3$, and $Fe(NO_3)_3 \cdot 9H_2O$. Appropriate amounts of the mixtures were dissolved in diluted nitric acid, co-precipitated, and then fired at 800 °C for 4 h. After being ground and mixed for several hours, in order to increase the contact area between particles, each mixture was pressed into pellet form under a pressure of 2.5 ton cm^{-2} and all the pellets were heated at 1000 °C for 8 h. After regrinding and repelleting, they were sintered at 1200 °C for 36 h under atmospheric air pressure and quenched.

2.2. X-ray powder diffraction and thermal analysis

X-ray diffraction studies of the powder samples were carried out with monochromatized CuK_α ($\lambda = 0.15418$ nm) radiation in the 2θ range from 15°–80°. The crystal system, lattice parameters, and reduced lattice volume of the unit cell were determined reasonably. In order to determine the change of the oxygen content in the samples, thermogravimetric analysis (TGA) was carried out from room temperature to 670 K under atmospheric air pressure with a quartz balance made by our group. However, there was no detectable change in oxygen content, which was consistent with the fact that, considering the stable electron configuration of La^{3+} and Ba^{2+} ions, the invariable oxidation state of iron ion was retained under the experimental conditions.

2.3. Chemical analysis

The oxidation state of iron at room temperature was determined by Mohr salt titration. The amount of Fe^{4+} ion, the oxygen vacancy, and the non-stoichiometric chemical formulae for the system were also determined.

2.4. Mössbauer effect

The Mössbauer spectra were recorded at room temperature using a spectrometer which consisted of a 308-channel pulse-height analyser. The source was $^{57}Co/Rh$ with 14.4 keV γ-radiation. The isomer shift, quadrupole splitting, and hyperfine field were determined relative to the spectrum of α-Fe.

2.5. Electrical conductivity

Electrical conductivities of the samples were measured using the four-probe d.c. technique in the temperature range 173–670 K under atmospheric air pressure. The electrical conductivities were calculated from Laplume's equation.

3. Results and discussion

3.1. X-ray powder diffraction

The X-ray powder diffraction pattern of the composition with $x = 0.00$ is assigned to orthorhombic symmetry on the basis of a distorted perovskite-type structure similar to $GdFeO_3$. The spectra for the compositions of $x = 0.25$, 0.50, and 0.75 make it possible to assign the compositions as simple cubic perovskite structure. The solid solution of the composition of the $x = 1.00$ has orthorhombic symmetry, which was previously assigned to $BaFeO_{2.60}$ by Shaplygin *et al.* [18]. In Table I, the observed d-values and intensities of diffraction lines for the composition with $x = 0.25$, as an example, are compared with those calculated from Miller indices assigned carefully, and $I = |F|^2 P(1+\cos^2\theta)/(\sin^2\theta\cos\theta)$, respectively. Agreement between observed and calculated values is quite good.

Lattice parameters, reduced lattice volume of the unit cell, and the crystal system, in accordance with the composition, are listed in Table II. According to our previous review [1], the volume of the unit cell of the ABO_3 system is affected by three factors: the ionic radius of the substituted ion in the A-site, oxygen

TABLE I Indexing of X-ray diffraction spectrum of the $Ba_{0.25}La_{0.75}FeO_{2.95}$ system

hkl	$d_{obs.}$ (nm)	$d_{cal.}$ (nm)	I/I_0 (obs.)	I/I_0 (cal.)
100	0.3937	0.3931	19.15	12.68
110	0.2779	0.2779	100.00	100.00
111	0.2269	0.2269	21.02	19.00
200	0.1965	0.1965	30.19	33.57
201	0.1758	0.1758	6.25	6.40
211	0.1604	0.1605	36.70	38.77
220	0.1389	0.1390	14.63	19.55
221	0.1311	0.1310	3.46	2.83
310	0.1243	0.1243	13.30	16.59

TABLE II Lattice parameters, reduced lattice volume, and crystal system for the $Ba_xLa_{1-x}FeO_{3-y}$ system

x	Lattice parameters (nm)			Reduced lattice volume (10^{-3} nm^3)	Crystal system
	a	b	c		
0.00	0.5558	0.5551	0.7834	60.43	Orthorhombic
0.25	0.3931	–	–	60.73	Cubic
0.50	0.3945	–	–	61.40	Cubic
0.75	0.3988	–	–	63.41	Cubic
1.00	0.5853	1.632	1.092	65.19	Orthorhombic

vacancy, and the formation of the mixed valence state of the B-site. The reduced lattice volume increases with the higher substitution of the Ba^{2+} (r(XII) = 0.161 nm) for the La^{3+} (r(XII) = 0.116 nm) [17] as shown in Fig. 1, despite the increasing oxygen vacancy and the substitution of the smaller Fe^{4+} (r(VI) = 0.0585 nm) for the larger Fe^{3+} (r(VI) = 0.0645 nm). Thus we conclude that the effect of ionic radius of the substituted ion at the A-site in our system is predominent.

3.2. Chemical analysis

The mole ratio of Fe^{4+} ion (τ value), the amount of oxygen vacancy (y value), and the non-stoichiometric chemical formula corresponding to each composition are listed in Table III. The composition of $x = 0.00$ or $LaFeO_{3.00}$ is a stoichiometric compound and the others are non-stoichiometric compounds. As shown in Fig. 2, the τ value increases with x value in the range, $0.00 \leqslant x \leqslant 0.75$ and thus the composition of $x = 0.75$ has the maximum τ value. However, the τ value decreases at the composition of $x = 1.00$ in which the formation of oxygen vacancies might be easier than the formation of the Fe^{4+} ion. The y value is increased steadily with increasing x value. The ordering of vacancies minimizes the lattice energy in accordance with the increase of oxygen vacancies. From the results of XRD analyses, we confirm that all the solid solutions containing oxygen vacancies, except the composition $x = 1.00$, shows no interactions between vacancies. Therefore, the vacancies are distributed randomly or disordered within the lattice.

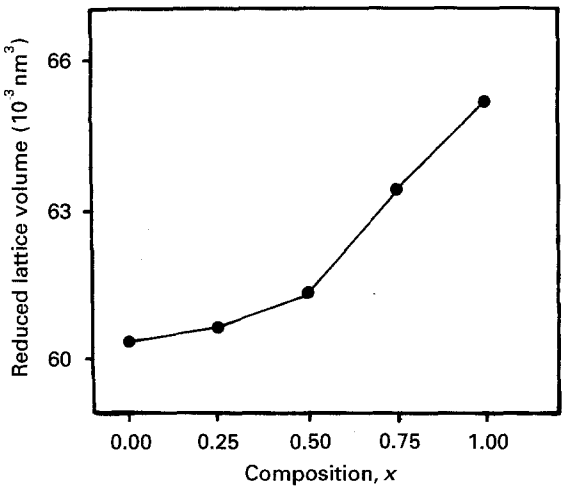

Figure 1 Plot of reduced lattice volume versus x value for the $Ba_xLa_{1-x}FeO_{3-y}$ system.

TABLE III x, τ, y values, and non-stoichiometric chemical formulae for the $Ba_xLa_{1-x}FeO_{3-y}$ system

x	τ	y	Chemical formula
0.00	0.00	0.00	$LaFe^{3+}O_{3.00}$
0.25	0.15	0.05	$Ba_{0.25}La_{0.75}Fe^{3+}_{0.85}Fe^{4+}_{0.15}O_{2.95}$
0.50	0.32	0.09	$Ba_{0.50}La_{0.50}Fe^{3+}_{0.68}Fe^{4+}_{0.32}O_{2.91}$
0.75	0.38	0.19	$Ba_{0.75}La_{0.25}Fe^{3+}_{0.62}Fe^{4+}_{0.38}O_{2.81}$
1.00	0.28	0.36	$BaFe^{3+}_{0.72}Fe^{4+}_{0.28}O_{2.64}$

3.3. Mössbauer effect

The Mössbauer spectra at room temperature for the compositions $x = 0.00$, 0.50, and 0.75 are shown in Figs 3–5. The Mössbauer spectra for the compositions $x = 0.25$ and 1.00 are not shown because of indistinguishable peaks. The Mössbauer parameters for the compositions $x = 0.00$, 0.50, and 0.75 in the $Ba_xLa_{1-x}FeO_{3-y}$ system are shown in Table IV. In Fig. 3, the Mössbauer spectrum of $LaFeO_3$ shows a series of six lines split under an internal magnetic field, which is characteristic of the antiferromagnetic compound below its Néel temperature. The isomer shift, 0.317 mm s^{-1}, and the hyperfine field, 541.8 kOe, are consistent with those of the Fe^{3+} valence state at the octahedral site. The asymmetry in the series of lines is indicative of electric field gradient at the site of the Fe^{3+} ion, which reflects zig-zag form of octahedral site axes, as in $GdFeO_3$. The Mössbauer spectrum of the composition $x = 0.50$, as shown in Fig. 4, is that of the paramagnetic compound. The paramagnetic spectrum can be fitted quite well using a model of the three

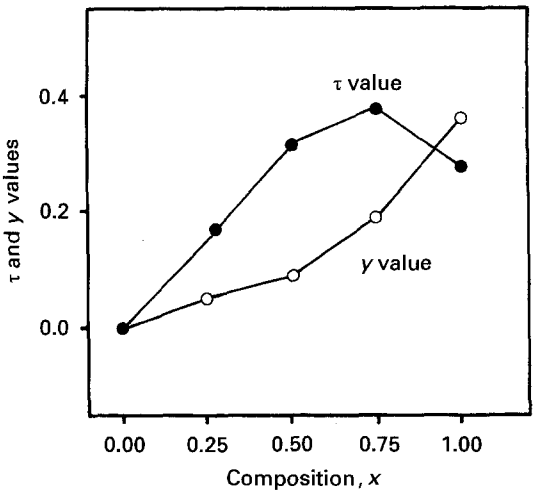

Figure 2 Plots of τ and y versus x for the $Ba_xLa_{1-x}FeO_{3-y}$ system.

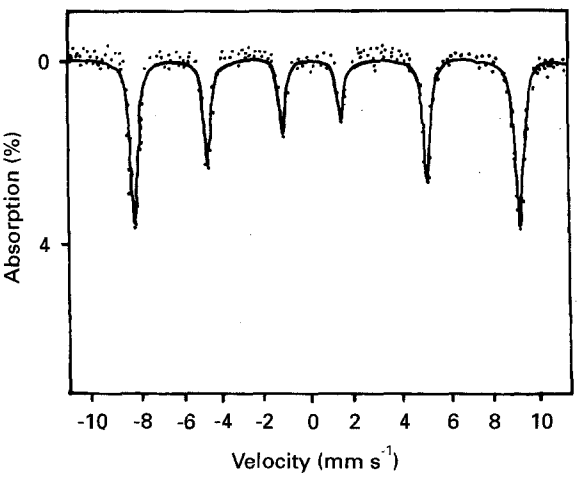

Figure 3 Mössbauer spectrum of the $LaFeO_{3.00}$ system.

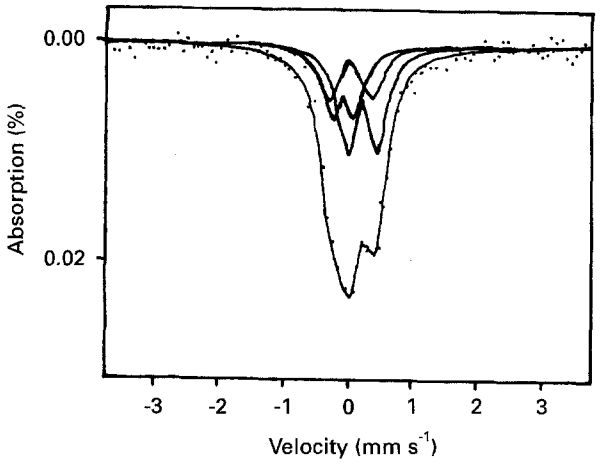

Figure 4 Mössbauer spectrum of the $Ba_{0.50}La_{0.50}FeO_{2.91}$ system.

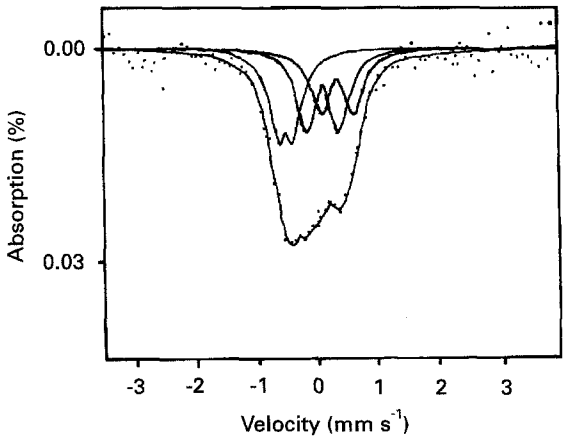

Figure 5 Mössbauer spectrum of the $Ba_{0.75}La_{0.25}FeO_{2.81}$ system.

TABLE IV Mössbauer parameters for the compositions of $x = 0.00$, 0.50, and 0.75 in the $Ba_xLa_{1-x}FeO_{3-y}$ system

x	Ion	Site	δ^a (mm s^{-1})	$\Delta E_q{}^b$ (mm s^{-1})	ΔH_n^c (kOe)
0.00	Fe^{3+}	Oh	0.317	0.208	541.8
0.50	Fe^{3+}	Oh	0.303	0.450	–
	Fe^{3+}	f.c	0.116	0.675	–
	Fe^{4+}	Oh	0.003	0.300	–
0.75	Fe^{3+}	Oh	0.414	0.527	–
	Fe^{3+}	f.c	0.188	0.527	–
	Fe^{3+}	Oh	−0.427	0.203	–

[a] δ, isomer shift.
[b] ΔE_q, quadrupole splitting.
[c] ΔH_n, hyperfine field.

series of overlapping symmetrical quadrupole doublets. The isomer shifts of 0.303 and 0.116 mm s^{-1} assign the two doublets to the Fe^{3+} ion; that of 0.003 mm s^{-1} makes it possible to assign the one doublet to the Fe^{4+} ion, as shown in Table IV. We suggest two models: a vacancy ordering system with tetrahedral and octahedral sites of iron ions, and a vacancy disordering system with five coordinated and octahedral sites of iron ions. Assuming the Fe^{4+} ion only at the octahedral site [19], we calculated the ratios of the sites in each model from the number of oxygen vacancies as shown in Table V. When we compare the observed and calculated values, the spectrum is explained in terms of the vacancy disordering system. The Mössbauer spectrum for the composition $x = 0.75$, as shown in Fig. 5, is the paramagnetic one with a series of six lines. The paramagnetic spectrum can be fitted using a complex model with three series of overlapping symmetrical quadrupole doublets. The isomer shifts of −0.427, 0.188 and 0.414 mm s^{-1} correspond to the octahedral Fe^{4+} ion, the five-coordinated Fe^{3+} ion, and the octahedral Fe^{3+} ion, respectively, as listed in Table V. The vacancy ordering model with tetrahedral sites is less favourable in both compositions, which is a different behaviour from the $(Ca, La)FeO_{3-y}$ and $(Sr, La)FeO_{3-y}$ systems, due to the larger barium ion. The Mössbauer spectra of the compositions of $x = 0.25$ and 1.00 are indistinct. It seems that the transition temperatures of magnetic ordering are at near room temperature. The higher transition temperature of the $x = 1.00$ is consistent with the orthorhombic structure assigned from X-ray diffraction analysis. According to the literature [12, 15, 20], in monoclinic and orthorhombic phases, the temperatures are above room temperature because of stronger Fe–O–Fe interaction.

TABLE V Relative ratios of the sites calculated in the vacancy ordering and vacancy disordering models and that observed

x	Vacancy ordering		Vacancy disordering		Obs. (%)
	Site	Calc. (%)	Site	Calc. (%)	
0.50	Oh(Fe^{4+})	32	Oh(Fe^{4+})	32	31
	Oh(Fe^{3+})	59	Oh(Fe^{3+})	50	46
	Td(Fe^{3+})	9	f.c.(Fe^{3+})	18	23
0.75	Oh(Fe^{4+})	38	Oh(Fe^{4+})	38	38
	Oh(Fe^{3+})	43	Oh(Fe^{3+})	24	27
	Td(Fe^{3+})	19	f.c.(Fe^{3+})	38	35

In general, the isomer shift of the Fe^{4+} ion decreases with increasing x values, but that of the octahedral Fe^{3+} ion increases. This is ascribed to the fact that the Fe^{4+} ion with higher charge and smaller ionic radius attracts neighbouring oxygen ions and the covalency between the Fe^{4+} ion and oxygen ion increases. In reverse, the Fe^{3+} ion neighbouring the Fe^{4+} ion has a decreasing covalency with oxygen ions. Because the quadrupole splitting results from the electrical field gradient at the nucleus of the iron ion, it reflects the asymmetry of the coordinator around the iron ion. The five-coordinated Fe^{3+} ion has the largest electrical field gradient. The antiferromagnetic behaviour of the $LaFeO_{3.00}$ can be described by a superexchange model in which the antiferromagnetic Fe^{3+}–O–Fe^{3+} interaction is predominent. However, the superexchange interaction collapses as a mixed valence of the iron ions and an oxygen vacancy are produced by the substitution of the Ba^{2+} ion for the La^{3+} ion [20]. The transition temperature of the magnetic ordering decreases in the series of the compositions from $x = 0.00$–0.75. That is, the temperatures for the compositions of $x = 0.00$, 0.25, 0.50, and 0.75 are above, near, below, and also below room temperature,

respectively. The transition temperature for $x = 1.00$, however, is near room temperature.

3.4. Electrical conductivity

The electrical conductivity measurement has been carried out in the temperature range 173–670 K under atmospheric air pressure as shown in Fig. 6. The activation energies of the conductivity are listed in Table VI for all the compositions in the given temperature ranges. The composition of $x = 0.00$ has a lower value of conductivity and a higher activation energy of conduction than those of the ferrites containing Fe^{4+} ion in the compositions $x \geqslant 0.25$. The mixed valence state between Fe^{3+} and Fe^{4+} ions leads to high conductivity. The conductivity of the $LaFeO_3$ can be explained by hopping of electrons between the Fe^{3+} and Fe^{4+} ions formed from oxygen vacancies or lanthanium vacancies entered slightly thermally [9]. The higher value of activation energy corresponds to the formation and migration energies of the conduction carrier.

For the series of compositions from $x = 0.25$–1.00, the conductivity is slightly increased with temperature as in a semiconductor behaviour. At a given temperature, even though the mole number of Fe^{4+} ions or the τ value increases with the order of $x = 0.25$, 1.00, 0.50, and 0.75, the conductivity increases with the order of $x = 1.00$, 0.25, 0.75, and 0.50, as shown in Table III and Fig. 6. The conductivity not only depends on the τ value but also on the number of oxygen vacancies. The vacancies serve as scattering centres to reduce the mobility or act as trapping sites to decrease the carrier concentration. For compositions of $x = 0.50$ and 0.75, they have similar τ values, but the mole number of oxygen vacancies is 0.09 in $x = 0.50$ and 0.19 in $x = 0.75$. The higher conductivity and lower activation energy of the $x = 0.50$ than of the $x = 0.75$ are due to larger number of oxygen vacancies in the $x = 0.75$ composition. The conductivity of $x = 0.75$ is higher than that of $x = 0.25$, which is consistent with the concentration of Fe^{4+} ions in both compositions. However, the larger number of oxygen vacancies in the composition of $x = 0.75$ increases the activation energy part for the mobility of the conduction carrier. The oxygen vacancy effect is mostly predominant in the composition of $x = 1.00$. Thus the conductivity and the activation energy are lowest and highest, respectively, in the ferrites containing Fe^{4+} ions. Such a change in electrical conductivity is due to electron hopping between Fe^{3+} and Fe^{4+} ions.

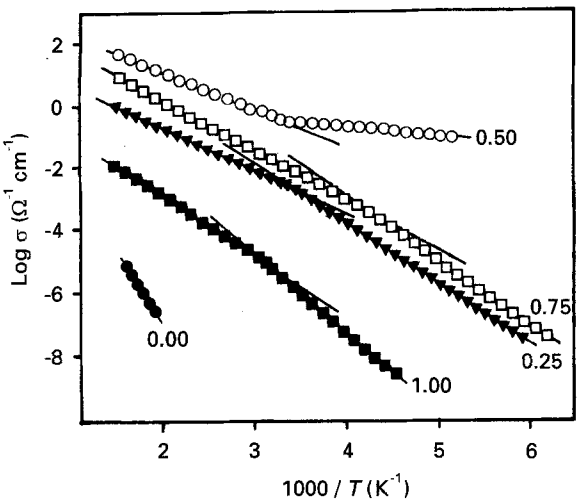

Figure 6 Plots of $\log\sigma$ versus $1000/T$ for the $Ba_xLa_{1-x}FeO_{3-y}$ system.

TABLE VI Activation energy of the electrical conductivity for the $Ba_xLa_{1-x}FeO_{3-y}$ system

x	Temperature (K)	Activation energy (eV)
0.00	550–562	1.14
0.25	296–450	0.28
	173–296	0.38
0.50	312–550	0.23
	173–261	0.06
0.75	245–600	0.32
	173–245	0.38
1.00	300–600	0.39
	173–300	0.53

The transition temperatures are 296 K for the composition of $x = 0.25$, the broad temperature range, 261–312 K, for $x = 0.50$, and 300 K for $x = 1.00$, as shown in Table VI and Fig. 6. For the compositions of $x = 0.25$ and 1.00, the transition points are in agreement with the magnetic ordering temperatures of the compositions.

Acknowledgement

This work was supported by a Yonsei University Faculty Research Grant for 1992.

References

1. C. H. YO, K. S. ROH, S. J. LEE, K. H. KIM and E. J. OH, *J. Kor Chem. Soc.* **35** (1991) 211.
2. C. H. YO, E. S. LEE and M. S. PYUN, *J. Solid State Chem.* **73** (1988) 411.
3. C. H. YO, S. J. LEE and S. H. CHANG, *J. Nat. Soc. Res. Inst.* **12** (1983) 65.
4. B. BUFFAT, G. DEMAZEAU, M. POUCHARD, J. M. DANCE and P. HAGENMULLER, *J. Solid State Chem.* **50** (1983) 33.
5. J. B. GOODENOUGH, *J. Phys. Chem. Solids* **6** (1958) 287.
6. V. G. BHIDE, D. S. RAJORIA, G. RAMA RAO and C. N. R. RAO, *Phys. Rev. B* **6** (1972) 1021.
7. M. EIBSCHÜTZ, S. SHTRIKMAN and D. TREVES, *Phys. Rev.* **156** (1967) 562.
8. C. BOCKEMA, F. VANDER WOUDE and G. A. SAWATZKY, *Phys. Rev. B* **11** (1975) 2705.
9. J. MIZUSAKI, T. SASAMOTO, W. R. CANNON and H. K. BOWEN, *J. Am. Ceram. Soc.* **65** (1982) 363.
10. *Idem, ibid.* **66** (1983) 247.
11. M. PARRAS, M. VALLET-REGI, J. M. GONZALEZ-CALBET and J. C. GRENIER, *J. Solid State Chem.* **83** (1989) 121.
12. P. K. GALLAGHER, J. B. MacCHESNEY and D. N. E. BUCHANAMN, *J. Chem. Phys.* **43** (1965) 516.
13. H. J. RICHTLER and K. A. HEMPEL, *J. Appl. Phys.* **64** (1988) 5980.

14. J. M. GONZALEZ-CALBET, M. PARRAS, M. VALLET-REGI and J. C. GRENIER, *J. Solid State Chem.* **86** (1990) 149.
15. A. J. JACOBSON, *Acta. Crystallogr.* **B32** (1976) 1087.
16. P. D. BATTLE, T. C. GIBB, P. LIGHTFOOT and M. MATSUO, *J. Solid State Chem.* **85** (1990) 38.
17. M. PARRAS, M. VALLET-REGI, J. M. GONZALEZ-CALBET, M. ALZRIO-FRANCO and J. C. GRENIER, *ibid.* **74** (1988) 110.
18. I. SHAPLYGIN, YA SHUBRT and A. ZAKHAROV, *Russ. J. Inorg. Chem.* (English Translation) **31** (1986) 1074.
19. A. WATTIAUX, J. C. GRENIER, M. POUCHARD and P. HAGENMULLER, *J. Electrochem. Soc.* **134** (1987) 1718.
20. T. C. GIBB and M. MATSUO, *J. Solid State Chem.* **81** (1989) 83.

Received 31 January
and accepted 24 August 1994